Proceedings of the
10th Graz Brain-Computer Interface Conference 2026
10.3217/978-3-99161-093-9-028

Finger abduction trajectory prediction from high-density ECoG

Axel Faes[1], Eva Calvo Merino[1], Mani Mirsaeedi[1], Anaïs Van Hoylandt[2], Elina Keirse[2], Tom Theys[2], Marc M. Van Hulle[1]

[1] KU Leuven - University of Leuven, Department of Neurosciences, Laboratory for Neuro- & Psychophysiology, B-3000 Leuven, Belgium

[2] KU Leuven - University of Leuven, Department of Neurosciences, Research Group Experimental Neurosurgery and Neuroanatomy, B-3000 Leuven, Belgium

E-mail: marc.vanhulle@kuleuven.com

ABSTRACT: A case study is conducted to demonstrate that not only finger flexion but also finger abduction trajectories can be decoded from high density electrocorticography (ECoG) recordings. Two patients, temporarily implanted with high-density ECoG grids as part of their clinical workup, performed three cued tasks: single finger flexion, finger abduction, and sign language alphabet gestures. The extended Block-Term Tensor Regression (eBTTR) model is trained on simultaneous ECoG and data glove recordings to predict continuous finger trajectories. Performance on the flexion task serves as a baseline for comparison with abduction decoding. The sign language task involves realistic, complex finger movements combining both flexion and abduction. We show that finger abduction trajectories can be decoded from ECoG with precision comparable to single finger flexion, even during sign language gestures that involve joint finger flexions and abductions. To our knowledge, this is the first demonstration that finger abduction trajectories can be decoded from ECoG.

INTRODUCTION

The field of Brain-Computer Interfaces (BCIs) has witnessed significant advancements in motor applications, particularly in restoring or replacing the function of lost or impaired body functions. Notable examples include the electrical stimulation of hand muscles and specific regions of the spinal cord involved in walking, as demonstrated by Lorach et al. [1]. Additionally, BCIs have proven effective in controlling prosthetic hands, arms, exoskeletons, and other effectors [2, 3, 4, 5]. In recent years, electrocorticography (ECoG) has garnered attention within the BCI research community. ECoG involves the placement of electrodes on the exposed cortical surface to record electrical activity. Compared to other implant types, ECoG offers a broader coverage of the cortical surface, enhanced long-term signal stability [6, 7], superior spatial resolution compared to electroencephalography (EEG) [8], and a more extensive spectral bandwidth with increased signal amplitude [9]. Various studies [10, 11, 12, 13, 14, 15, 16] have highlighted the potential of ECoG signals from the primary motor cortex in decoding continuous arm trajectories, as they exhibit distinctive motor-related spatio-temporo-spectral patterns [17, 11, 18]. Nonetheless, decoding rapid and coordinated finger movements, such as object grasping and hand gestures, remains a challenge, necessitating further algorithmic developments. Pioneering work by Kubanek et al. [19] focused on continuous decoding of individual finger flexions and extensions using local motor potentials (LMP) and spectral amplitudes across five frequency bands.

Previous research has demonstrated successful decoding of finger flexion movements from ECoG signals [16, 20, 21, 22, 23, 24, 25]. Block-Term Tensor Regression (BTTR), as detailed in [26] and [27], was recently introduced for ECoG-based finger flexion decoding. The main algorithmic principle behind BTTR is Tucker decomposition. Block-Term refers to a deflation scheme that generates blocks with varying multilinear Tucker ranks. Originally, BTTR predicted single finger trajectories only, but extended BTTR (eBTTR) lifted this limitation so that coordinated finger movements could be predicted, including finger co-activations i.e. unintentional finger movements [28]. While, in principle, one could stack BTTR models of individual fingers, it will fall short in addressing the temporal overlap and spatial sparsity ECoG signals exhibit during coordinated finger flexions [29].

The aforementioned studies focused on finger flexions, which is useful for applications such as grasping a cup. However, when aiming for restoring hand dexterity, finger abduction becomes important as well. Although the accurate prediction of finger abduction trajectories from (high-density) ECoG could have a significant impact on the development of hand motor BCIs, it has received less attention.

Some studies tangentially refer to finger abduction as part of two-dimensional finger movements. In [30] an intracortical BCI was developed to decode attempted handwriting movements from micro-electrode implants in a paralyzed individual's hand knob area. Patients were instructed to imagine they were holding a pen and were writing on (ruled) paper. In [13] middle finger movements were decoded from ECoG to control a

10.3217/978-3-99161-093-9-028

cursor in two dimensions. These movements involve both finger flexion and abduction. However, the said studies do not directly investigate the decoding of finger abduction.

Hu and colleagues ([31]) investigated finger movement recognition via high-density surface electromyography (HD-sEMG). Their study involved 20 healthy subjects and, using a 22-sensor dataglove, had them perform various finger movements including finger flexion and finger abduction. They found that finger abduction could be decoded similarly to finger flexions.

In order to investigate finger abductions from high-density ECoG, a case study was conducted involving subjects performing three different tasks: a cued single finger flexion task, a cued sign language gesture alphabet task, and a cued finger abduction task. The cued single finger flexion task served as a reference to compare the performance of finger flexion decoding with finger abduction decoding. By analyzing the ECoG data, the study aimed to determine if finger abductions could be decoded with a similar level of accuracy as finger flexions. Furthermore, the sign language gesture alphabet task provided an opportunity to investigate the decoding of complex finger movements that involve both flexions and abductions. The dataset used in this study consisted of ECoG recordings from two patients who performed all gestures of the Flemish Sign Language Alphabet, as well as explicit finger abduction movements. The eBTTR algorithm was employed as the decoding model [28]. The findings demonstrate that single finger abductions as well as complex hand gestures from the Sign Language Alphabet can be decoded from ECoG. The results indicate that finger abductions can be decoded with a similar level of precision as single finger flexions. This suggests that ECoG signals hold promise for predicting finger abduction trajectories, expanding the potential applications of BCIs for controlling hand prosthetics and exoskeletons and for promoting neurorehabilitation.

MATERIALS AND METHODS

Dataset and tasks

The dataset originates from two patients undergoing treatment of refractory neuropathic facial pain with epidural electrocorticography (ECoG) grids placed on part of the somatosensory and motor cortex. Ethics approval for this study was granted by the Ethics Committee Research UZ/KU Leuven (EC Research). The first patient had an epidural ECoG grid implanted on the right hand-knob area, while the second patient had a grid placed on the left subcentral gyrus and Broca area, and one on the right hand-knob area (refer to Table 1, and Figures 1-3).

Table 1: Patient Information Leuven dataset

	Subject 1	Subject 2
Age	58	41
Gender	Female	Female
Handedness	Right	Right
Region of pain	Trigeminus neuralgia (left)	Temporomandibular joint disorder, bilateral pain mostly in jaws.
Number of grids	1	2
Type of grid	Inc Medtronic Inc Specify® SureScan® MRI 5-6-5 grid (in-line spacing 4.5 mm, row spacing 1.0 mm, electrode size 1.5 mm x 4.0 mm)	2X Medtronic Inc Specify® SureScan® MRI 5-6-5 grid, in-line spacing 4.5 mm, row spacing 1.0 mm, electrode size 1.5 mm x 4.0 mm
Implanted hemisphere	Right	Left and right
ECoG Grid location	Medial frontoparietal, covering M1 and S1, face and lip area	Left: Lateral frontoparietal, inferior parietal cortex and Broca (Brodmann inferior area 44, inferior frontal gyrus pars opercularis left), Right: Medial frontoparietal, covering M1, S1 hand knob & PMDc
Total number of included electrodes	16	32
Number of electrodes over M1	3	Left: 2, Right: 3
Number of electrodes over S1	4	Left: 5, Right: 4

 10.3217/978-3-99161-093-9-028

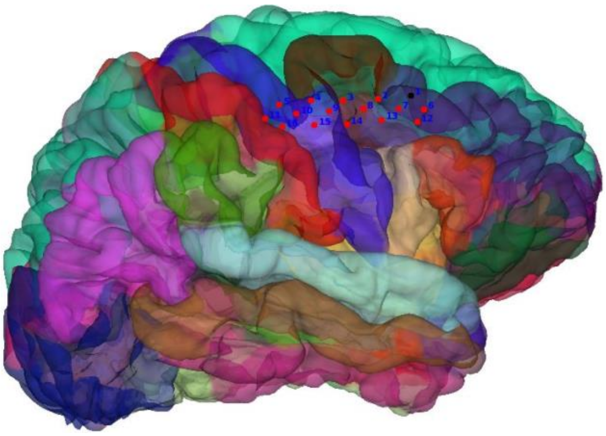

Figure 1: Visual representation of the ECoG grid placement on the right hand-knob area of subject 1.

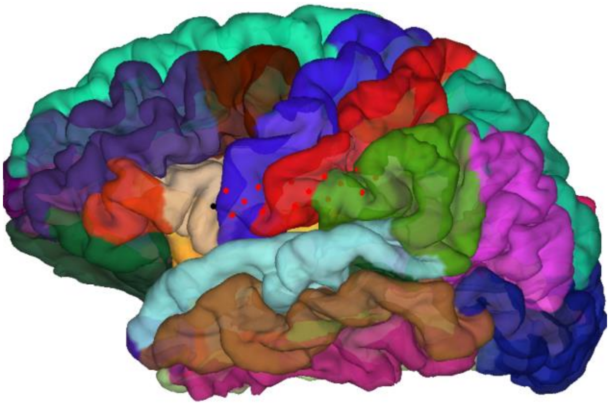

Figure 2: Visual representation of the ECoG grid placement on the left subcentral gyrus and Broca area of subject 2.

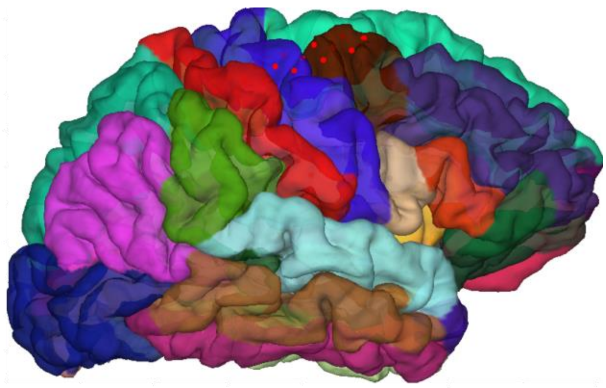

Figure 3: Visual representation of the ECoG grid placement on the right hand-knob area of subject 2.

Three tasks were performed (subject 2 participated in tasks 2 and 3 only). Task 1 involved single finger movements, in which case subject 1 received a cue to start flexing a specific finger with its trajectory measured using a 5DT 14 Ultra data glove (5DT Inc., Irvine, USA). On average, subject 1 was instructed to flex the prompted finger once for 1 to 2 seconds, followed by a rest period lasting 2 seconds. A total of 150 trials were conducted in a single session lasting 600 seconds, with 30 trials for each finger. In Task 2, both subjects were cued to replicate each of the 26 letters of the Flemish sign language alphabet, cued in randomized order using a hand avatar, with the finger trajectories being measured using the said data glove. Given the location of the experiment in Flanders (Belgium), the Flemish Sign Language alphabet was utilized. In Task 3, the two subjects were cued again using a hand avatar, to perform a specific finger abduction pattern, i.e., spreading of two adjoining fingers as wide as possible, again with the finger trajectories being recorded using the same data glove. A total of 120 trials were conducted in a single session lasting 480 seconds, with 30 trials for each abduction. On average, subjects were directed to perform the specified abduction (using an avatar) once for 1 to 2 seconds, followed by a rest period lasting 2 seconds.

Processing

Notch filters, centered at 50 and 100 Hz, were employed to eliminate power line noise. Subsequently, a visual inspection of the data was conducted to identify and eliminate faulty channels. A channel was flagged as problematic if it displayed an unstable or unchanging signal. Following this, Common Average Reference (CAR) re-referencing was applied by subtracting the average signal from all signals [32]. Finally, the ECoG signals were structured into a 4th-order ECoG tensor $\underline{\mathbf{X}} \in \mathrm{R}^{\text{Samples}\times\text{Channels}\times\text{Frequencies}\times\text{Time}}$. In this representation, Samples corresponds to the size of vector Y (recorded from the data glove), and Channels reflects the number of electrodes remaining after the removal of faulty channels. Frequencies encompasses 16 components, including 15 gamma band powers and the local motor potential (LMP). The gamma band powers were extracted in the 60 to 130 Hz range (high-frequency bands) using 10 Hz frequency bands with 5 Hz overlap, by bidirectional third-order Butterworth band-pass filters [33]. The LMP was determined by extracting amplitudes in the 0.1 to 1.5 Hz range. Time comprises 10 instances derived from the most recent 1-second epoch, achieved by downsampling each of the 16 band-pass filtered ECoG signals to 10 Hz. The preprocessing steps are as follows:

- Normalize (i.e., z-score) data glove trajectories independently for each finger $\mathrm{Y} \in \mathrm{R}^{\text{Samples}\times\text{Fingers}}$.
- Apply epoch selection for each channel using the past second for band-pass filtering, followed by a downsampling to 10 Hz. This process yields the frequency and time dimensions for each sample and channel.
- Normalize (i.e., z-score) the tensor according to the channel and frequency bands of the training set, with the same parameters applied to the test set.
- Merge the channel matrices into $\underline{\mathbf{X}} \in \mathrm{R}^{\text{Samples}\times\text{Channels}\times\text{Frequencies}\times\text{Time}}$.

The resulting preprocessed data is then utilized in extended Block Term Tensor Regression (eBTTR), a regression model specifically designed to accommodate the multilinear nature of human intracranial recordings

 10.3217/978-3-99161-093-9-028

(see [28] for a complete description of the decoder). The model relies on recursive Tucker decomposition combined with automatic component extraction [27, 28]. A 5-fold cross-validation approach was used to determine the optimal number of Tucker blocks. For each of the three tasks, a separate eBTTR model is trained. This also allows for cross-testing, i.e. use an eBTTR model trained on task 1 (single finger) to decode task 2 (joint finger).

Model performance is expressed in terms of the Pearson correlation coefficient between the data glove recorded finger trajectories and the predicted ones. The test dataset was partitioned into five non-overlapping blocks. For assessing the significance of differences in average accuracies across various fingers and subjects, we employed the Wilcoxon signed-rank test (two-tailed) [34]; a result with a p-value smaller than 0.05 was considered significant.

RESULTS AND DISCUSSION

Per-task analysis

Table 2 summarizes the finger flexion results of Task 1 and 2. Note that Task 1 was performed by subject 1 only. Task 2 considers all gestures of the sign language alphabet, thus going beyond the selection of 4 gestures of the Utrecht experiment [35].

For Task 1, Subject 1 shows higher correlation coefficients for the thumb, index and ring fingers compared to the other fingers. For task 2, both subjects exhibit varying correlation coefficients across different fingers, with mostly higher coefficients for Subject 2.

Table 2: Pearson correlation coefficients of cued single finger movement and finger gesture trajectories.

Methods	Thumb	Index	Middle	Ring	Pinky
Single Finger subj.1	0.31±.05	0.45±.07	0.12±.04	0.23±.02	0.16±.01
Finger gesture subj.1	0.42±.05	0.32±.07	0.38±.04	0.23±.02	0.12±.01
Finger gesture subj.2	0.32±.05	0.46±.07	0.49±.04	0.32±.02	0.33±.01

Table 3 summarizes the finger abduction results of Task 3. The results reveal distinctive correlation patterns for specific finger pairs, with Subject 2 exhibiting overall stronger correlations, especially for the Middle-Ring and Ring-Pinky pairs. Comparing the Task 2 (finger gestures), the same fingers flexed individually also yield stronger correlations. It seems, thus, that finger flexions and finger abductions yield similar decoding accuracies. The exception is the Thumb as it features the lowest abduction decoding accuracy for both subjects but a good flexion decoding performance during finger gesture movements. We expect that this is due to the difficulty to accurately gauge Thumb abductions vs. flexions with the data glove (the abduction of the listed fingers pairs is measured by dedicated sensors unlike the thumb).

Table 3: Pearson correlation coefficients of cued finger abduction movement

Subject	Thumb-Index	Index-Middle	Middle-Ring	Ring-Pinky
Subj. 1	0.14±.05	0.32±.07	0.28±.04	0.22±.01
Subj. 2	0.04±.05	0.36±.08	0.37±.04	0.37±.01

Cross-task analysis

Since subject 1 performed both Task 1 and 2, a cross-task analysis was performed. Hereby, an eBTTR model was trained on the data of Task 1 and tested on Task 2 and vice-versa. The results are summarized in Table 4. The performance of the model trained on single finger movements is significantly lower compared to the performance of the model trained on joint finger movements (see Table 2).

Table 4: Pearson correlation coefficients of cued single finger movement and finger gesture trajectories (for Subject 1)

Methods	Thumb	Index	Middle	Ring	Pinky
Train T1/Test T2	0.22±.06	0.12±.02	0.21±.05	0.08±.02	0.09±.02
Train T2/Test T1	0.28±.03	0.27±.04	0.07±.01	0.21±.02	0.15±.01

CONCLUSION

We presented a comprehensive investigation into the prediction of finger abduction trajectories from high-density ECoG data. The study demonstrates the feasibility of decoding finger abductions using the eBTTR algorithm and shows a decoding performance that is comparable to finger flexion except for the thumb, possibly due to technical aspects of the used data glove. These findings could contribute to the development of hand prosthetics and exoskeletons and to hand neurorehabilitation.

ACKNOWLEDGEMENTS

This work is supported by research grants received from Horizon Europe's Marie Sklodowska-Curie Action (grant agreement No. 101118964), Horizon 2020 research and innovation programme under grant agreement No. 857375, the special research fund of the KU Leuven (C24/18/098), the Belgian Fund for Scientific Research -- Flanders (G0A4321N, G0C1522N, G031426N, 1102925N), and the Hercules Foundation (AKUL 043).

REFERENCES

[1] Henri Lorach, Andrea Galvez, Valeria Spagnolo, Felix Martel, Serpil Karakas, Nadine Intering, Molywan Vat, Olivier Faivre, Cathal Harte, Salif Komi, et al. Walking naturally after spinal cord injury using a brain–spine interface. Nature, pages 1–8, 2023

[2] Leigh R Hochberg, Mijail D Serruya, Gerhard M Friehs, Jon A Mukand, Maryam Saleh, Abraham H Caplan, Almut Branner, David Chen, Richard D Penn, and John P Donoghue. Neuronal ensemble control of prosthetic devices by a human with tetraplegia. Nature, 442(7099):164–171, 2006

[3] Jennifer L Collinger, Brian Wodlinger, John E Downey, Wei Wang, Elizabeth C Tyler-Kabara, Douglas J Weber, Angus JC McMorland, Meel Velliste, Michael L Boninger, and Andrew B

10.3217/978-3-99161-093-9-028

Schwartz. High-performance neuroprosthetic control by an individual with tetraplegia. The Lancet, 381(9866):557–564, 2013

[4] Leigh R Hochberg, Daniel Bacher, Beata Jarosiewicz, Nicolas Y Masse, John D Simeral, Joern Vogel, Sami Haddadin, Jie Liu, Sydney S Cash, Patrick Van Der Smagt, et al. Reach and grasp by people with tetraplegia using a neurally controlled robotic arm. Nature, 485(7398):372–375, 2012

[5] B Wodlinger, JE Downey, EC Tyler-Kabara, AB Schwartz, ML Boninger, and JL Collinger. Ten-dimensional anthropomorphic arm control in a human brain- machine interface: difficulties, solutions, and limitations. Journal of neural engineering, 12(1):016011, 2014

[6] Wei Wang, Jennifer L Collinger, Alan D Degenhart, Elizabeth C Tyler-Kabara, Andrew B Schwartz, Daniel W Moran, Douglas J Weber, Brian Wodlinger, Ramana K Vinjamuri, Robin C Ashmore, et al. An electrocorticographic brain interface in an individual with tetraplegia. PloS one, 8(2):e55344, 2013

[7] Ewan S Nurse, Sam E John, Dean R Freestone, Thomas J Oxley, Hoameng Ung, Samuel F Berkovic, Terence J O'Brien, Mark J Cook, and David B Grayden. Consistency of long-term subdural electrocorticography in humans. IEEE Transactions on Biomedical Engineering, 65(2):344–352, 2017

[8] Kai J Miller, Larry B Sorensen, Jeffrey G Ojemann, and Marcel Den Nijs. Power-law scaling in the brain surface electric potential. PLoS Comput Biol, 5(12):e1000609, 2009

[9] Richard J Staba, Charles L Wilson, Anatol Bragin, Itzhak Fried, and Jerome Engel Jr. Quantitative analysis of high-frequency oscillations (80–500 hz) recorded in human epileptic hippocampus and entorhinal cortex. Journal of neurophysiology, 88(4):1743–1752, 2002

[10] Zenas C Chao, Yasuo Nagasaka, and Naotaka Fujii. Long-term asynchronous decoding of arm motion using electrocorticographic signals in monkey. Frontiers in neuroengineering, 3:3, 2010

[11] Leigh R Hochberg Tonio Ball, Markus Kern, Isabella Mutschler, Ad Aertsen, and Andreas Schulze-Bonhage. Signal quality of simultaneously recorded invasive and non-invasive eeg. Neuroimage, 46(3):708–716, 2009

[12] Jeroen CW Siero, Dora Hermes, Hans Hoogduin, Peter R Luijten, Nick F Ramsey, and Natalia Petridou. Bold matches neuronal activity at the mm scale: A combined 7 t fmri and ecog study in human sensorimotor cortex. Neuroimage, 101:177–184, 2014

[13] Leigh R Hochberg Gerwin Schalk, Kai J Miller, Nicholas R Anderson, J Adam Wilson, Matthew D Smyth, Jeffrey G Ojemann, Daniel W Moran, Jonathan R Wolpaw, and Eric C Leuthardt. Two dimensional movement control using electrocorticographic signals in humans. Journal of neural engineering, 5(1):75, 2008

[14] Takufumi Yanagisawa, Masayuki Hirata, Youichi Saitoh, Haruhiko Kishima, Kojiro Matsushita, Tetsu Goto, Ryohei Fukuma, Hiroshi Yokoi, Yukiyasu Kamitani, and Toshiki Yoshimine. Electrocorticographic control of a prosthetic arm in paralyzed patients. Annals of neurology, 71(3):353–361, 2012

[15] Elizabeth A Felton, J Adam Wilson, Justin C Williams, and P Charles Garell. Electrocorticographically controlled brain–computer interfaces using motor and sensory imagery in patients with temporary subdural electrode implants: report of four cases. Journal of neurosurgery, 106(3):495–500, 2007

[16] Alim Louis Benabid, Thomas Costecalde, Andrey Eliseyev, Guillaume Charvet, Alexandre Verney, Serpil Karakas, Michael Foerster, Aurélien Lambert, Boris Morinière, Neil Abroug, et al. An exoskeleton controlled by an epidural wireless brain–machine interface in a tetraplegic patient: a proof-of-concept demonstration. The Lancet Neurology, 18(12):1112–1122, 2019

[17] Nicholas R Anderson, Tim Blakely, Gerwin Schalk, Eric C Leuthardt, and Daniel W Moran. Electrocorticographic (ecog) correlates of human arm movements. Experimental brain research, 223(1):1–10, 2012

[18] David T Bundy, Mrinal Pahwa, Nicholas Szrama, and Eric C Leuthardt. Decoding three-dimensional reaching movements using electrocorticographic signals in humans. Journal of neural engineering, 13(2):026021, 2016

[19] Kubanek, Kai J Miller, Jeffrey G Ojemann, Jonathan R Wolpaw, and Gerwin Schalk. Decoding flexion of individual fingers using electrocorticographic signals in humans. Journal of neural engineering, 6(6):066001, 2009

[20] Qibin Zhao, Cesar F Caiafa, Danilo P Mandic, Zenas C Chao, Yasuo Nagasaka, Naotaka Fujii, Liqing Zhang, and Andrzej Cichocki. Higher order partial least squares (hopls): a generalized multilinear regression method. IEEE transactions on pattern analysis and machine intelligence, 35(7):1660–1673, 2012

[21] Andrey Eliseyev and Tetiana Aksenova. Penalized multi-way partial least squares for smooth trajectory decoding from electrocorticographic (ecog) recording. PloS one, 11(5):e0154878, 2016

[22] Rémi Flamary and Alain Rakotomamonjy. Decoding finger movements from ecog signals using switching linear models. Frontiers in neuroscience, 6:29, 2012

[23] Nanying Liang and Laurent Bougrain. Decoding finger flexion from band-specific ecog signals in humans. Frontiers in neuroscience, 6:91, 2012.

[24] Zuoguan Wang, Qiang Ji, Kai J Miller, and Gerwin Schalk. Decoding finger flexion from electrocorticographic signals using a sparse gaussian process. In 2010 20th International conference on pattern recognition, pages 3756–3759. IEEE, 2010

[25] Ziqian Xie, Odelia Schwartz, and Abhishek Prasad. Decoding of finger trajectory from ecog using deep learning. Journal of neural engineering, 15(3):036009, 2018

[26] Flavio Camarrone, Mariana P Branco, Nick F Ramsey, and Marc M Van Hulle. Accurate offline asynchronous detection of individual finger movement from intracranial brain signals using a novel multiway approach. IEEE Transactions on Biomedical Engineering, 68(7):2176–2187, 2020

[27] Axel Faes, Flavio Camarrone, and Marc M Van Hulle. Single finger trajectory prediction from intracranial brain activity using block-term tensor regression with fast and automatic component extraction. IEEE Transactions on Neural Networks and Learning Systems, submitted 2022

[28] A Faes and MM Van Hulle. Finger movement and coactivation predicted from intracranial brain activity using extended block-term tensor regression. Journal of Neural Engineering, 19(6):066011, 2022

[29] Gang Pan, Jia-Jun Li, Yu Qi, Hang Yu, Jun-Ming Zhu, Xiao-Xiang Zheng, Yue-Ming Wang, and Shao-Min Zhang. Rapid decoding of hand gestures in electrocorticography using recurrent neural networks. Frontiers in neuroscience, 12:555, 2018

[30] Francis R Willett, Donald T Avansino, Leigh R Hochberg, Jaimie M Henderson, and Krishna V Shenoy. High-performance brain-to-text communication via handwriting. Nature, 593(7858):249–254, 2021

[31] Xuhui Hu, Aiguo Song, Jianzhi Wang, Hong Zeng, and Wentao Wei. Finger movement recognition via high-density electromyography of intrinsic and extrinsic hand muscles. Scientific Data, 9(1):373, 2022

[32] Collin D Binnie. Clinical neurophysiology: EEG, paediatric techniques and applications, neurophysiology, special volume 2. Elsevier Health Sciences, 2003

[33] Ledyard R Tucker. Some mathematical notes on three-mode factor analysis. Psychometrika, 31(3):279–311, 1966

[34] Frank Wilcoxon. Individual comparisons by ranking methods. In Breakthroughs in statistics, pages 196–202. Springer, 1992

[35] Martin G Bleichner, Zachary V Freudenburg, Johannus Martijn Jansma, Erik J Aarnoutse, Mariska J Vansteensel, and Nick Franciscus Ramsey. Give me a sign: decoding four complex hand gestures based on high-density ecog. Brain Structure and Function, 221:203–216, 2016